Ripple Frequency Determined via a Novel Algorithm Is Associated With Atrial Fibrillation Termination and Freedom From Atrial Fibrillation

Daniel P. Melby, MD,* Venkatakrishna N. Tholakanahalli, MD,†‡ Refael Itah, MD, PhD,§ Raed Abdelhadi, MD,* Jay Sengupta, MD,* Charles C. Gornick, MD,* JoEllyn Moore, MD, FHRS,* Manjunath Pai, MD,* David G. Benditt, MD‡

*From the *Minneapolis Heart Institute and Foundation, Minneapolis, Minnesota, †VA Medical Center, Minneapolis, Minnesota, ‡University of Minnesota Medical School, Minneapolis, Minnesota, and §Biosense Webster, Haifa, Israel.*

BACKGROUND Persistent atrial fibrillation (AF) is a complex arrhythmia, and attaining freedom from AF with ablation has been challenging.

OBJECTIVES This study evaluated a novel CARTO software algorithm based on the CARTO Ripple map for AF termination and 18-month freedom from AF.

METHODS Consecutive patients who underwent first-time ablation for persistent AF were included. A high-density Ripple map was created using a Pentaray catheter. Following PVI, ablation was performed at locations with rapid Ripple activations, a protocol previously described by us. Patients were followed for 18 months to assess rhythm outcomes. A retrospective analysis was performed using the CARTO Ripple frequency software algorithm. The Ripple frequency algorithm quantifies amplitude changes in the bipolar electrogram.

RESULTS A total of 115 AF maps were analyzed from 84 patients (mean age 65.9 years, 63.1% men). The top quartile of Ripple frequency corresponded to a visual reference with 96.7% sensitivity and 91.1% specificity. AF terminated during ablation in 88.1% of patients: pulmonary vein antrum alone (14.9%) or pulmonary vein plus nonantral sites (85.1%). The top quartile of Ripple frequency was present in nonantral areas associated with AF termination with 90.2% sensitivity and 86.5% specificity. After 14.0 ± 6.5 months and 1.2 ± 0.4 ablations, 78 (92.9%) of 84 patients were free of AF, and 79.8% were free of any atrial arrhythmia.

CONCLUSION A novel algorithm for automated analysis of CARTO Ripple frequency demonstrated good sensitivity and specificity for detecting atrial regions in persistent AF in which ablation is associated with frequent AF termination and freedom from AF during follow-up.

KEYWORDS Persistent atrial fibrillation; Ablation; Ripple map; Electroanatomic map; Ripple frequency; Atrial fibrillation ablation

(Heart Rhythm O2 2022;■:1–8)

Atrial fibrillation (AF) is the most common sustained cardiac arrhythmia, with a lifetime risk estimated between 21% and 33% based on retrospective analysis.[1] Medical therapy alone often fails to control symptoms adequately, and ablation is performed to improve outcomes. Pulmonary vein isolation (PVI) remains the cornerstone of ablation for paroxysmal and persistent AF.[2,3] In paroxysmal AF, PVI with optimal contact-force radiofrequency or second-generation cryoballoon ablation results in approximately 80% 1-year freedom from AF.[4–6] In persistent AF (defined as continuous AF beyond 7 days' duration), PVI alone has a lower success, perhaps due to non-PV drivers.[7,8] Both experimental[9,10] and clinical[11–13] findings support the hypothesis that localized drivers maintain AF. In persistent AF, ablation of localized drivers has been demonstrated in some studies to improve freedom from AF.[12,13]

Ripple map is a software feature of the CARTO 3 electroanatomic mapping system (Biosense Webster, Irvine, CA) that graphically displays bipolar electrograms (Figure 1). This visual marker shows depolarization frequency, electrogram fractionation, and voltage. The Ripple display corresponds directly to the recorded bipolar electrogram, with no interpolation between points or other processing. Using this methodology, it is possible to visually assess all recorded electrograms within a cardiac chamber over extended time intervals. Our previous study found that high-frequency Ripple activation (HFRA) was associated with regions of spatiotemporal dispersion, and ablation of HFRA was associated with improved freedom from AF.[14]

Address reprint requests and correspondence: Dr Daniel P. Melby, 920 East 28th Street, Minneapolis, MN 55407. E-mail address: Daniel.melby@allina.com.

2666-5018/

https://doi.org/10.1016/j.hroo.2022.09.013

KEY FINDINGS

- The novel Ripple frequency algorithm corresponded to a visual reference with sensitivity and specificity of over 90%.
- The top quartile of Ripple frequency was present in nonantral areas associated with atrial fibrillation termination with 90.2% sensitivity and 86.5% specificity.
- Using a Ripple ablation approach, after 14.0 ± 6.5 months and 1.2 ± 0.4 ablations, 92.9% of patients were free of atrial fibrillation and 79.8% were free of any atrial arrhythmia.
- These findings support a potential association between Ripple frequency and critical areas of the atrium necessary for atrial fibrillation maintenance and possible recurrence.

This study aimed to evaluate a novel CARTO 3 software algorithm based on the CARTO Ripple map to identify high Ripple frequency locations and the relationship of these sites to AF termination and 18-month freedom from AF recurrence.

Methods

This study was a single-center retrospective evaluation of 84 consecutive patients from November 2016 to September 2021 who underwent first-time ablation for persistent AF. Patients had documented continuous AF by electrocardiography, Holter monitor, or implanted device for >7 days and <1 year. All patients underwent AF ablation using a Ripple map–guided approach.[14] Study participants were 18 years of age or older. Institutional Review Board approval was obtained, and all patients consented to research participation. The research reported in this paper adhered to the Helsinki Declaration guidelines.

Ripple Map–Guided Protocol and Mapping

To facilitate Ripple-based mapping, all patients in normal sinus rhythm (NSR) at baseline underwent AF induction with atrial burst pacing from the coronary sinus starting at 300 ms with a minimum of 200 ms. There was no predetermined burst pacing duration for the initial induction of AF. The left atrial (LA) anatomy was constructed using a Pentaray catheter (2-6-2 mm electrode spacing; Biosense Webster). Time continuous point acquisition of the entire LA chamber was performed with the Pentaray catheter using the Confidense algorithm (CARTO 3; Biosense Webster). Electroanatomic point density was set at 1 mm to diminish the variability in regional point clustering, which can be observed with alterations in Pentaray catheter movement speed. Electrode stability (a CARTO 3 Confidense feature that prevents point acquisition when electrode distance motion is above the threshold) was set at 3 mm to reduce catheter movement–induced electrogram artifact. The catheter was held stable for a minimum of 2.5 seconds. Continuous electrogram recording was performed over a minimum of 10 minutes. A minimum of 1500 bipolar electrogram points with

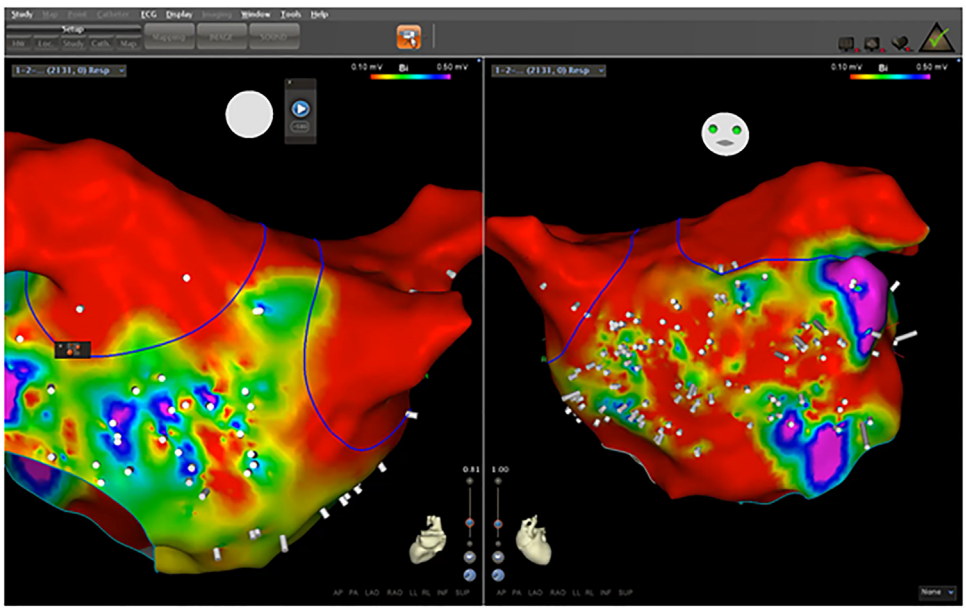

Figure 1 Example of Ripple map during sustained atrial fibrillation after pulmonary vein isolation. Color shading represents bipolar voltage displayed on the anatomic map with a range of 0.1 mV (red) to 0.5 mV (purple). White Ripple bars representing the bipolar electrograms are shown perpendicular to the map surface with the size corresponding to the bipolar voltage. A total of 2,131 points were acquired for this map with even distribution across the atrium. Some regions show no Ripple bars, indicating no depolarization at that location, rather than a lack of point acquisition. Analysis of this map demonstrated a high-frequency Ripple activation site with continuous high-frequency activation on the left atrial septum. Ablation of this location resulted in atrial fibrillation termination to normal sinus rhythm.

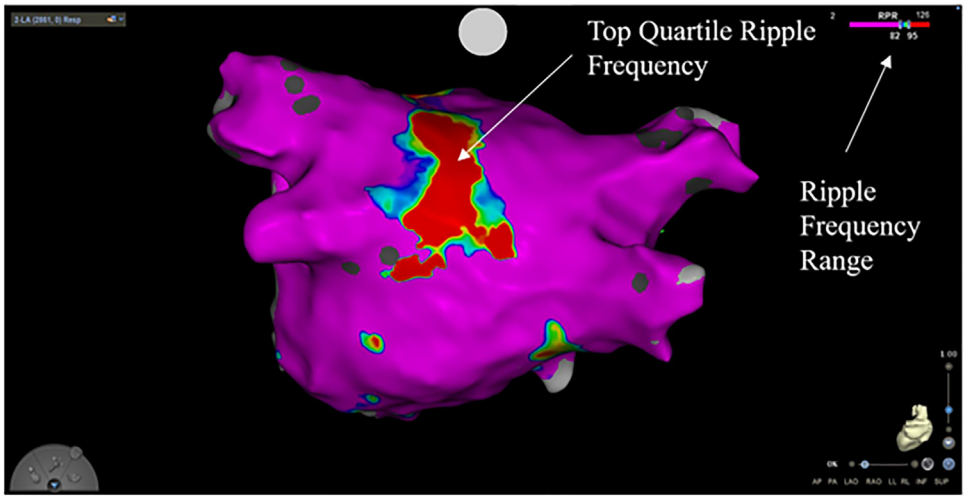

Figure 2 Example of Ripple frequency map obtained during sustained atrial fibrillation. Color shading represents the Ripple frequency. The Ripple frequency range in this example was 2 to 125 per second. The red color represents Ripple frequency more than 75% above the maximum (in this case, 95 per second). The purple color represents Ripple frequency <65% of the maximum (in this case, 82 per second). A total of 2861 points were acquired for this map with even distribution across the atrium. Analysis of this map demonstrated a large region of high Ripple frequency at the confluence of the left posterior pulmonary vein antrum and posterior wall. Ablation of this location resulted in atrial fibrillation termination to normal sinus rhythm.

equal electrogram density at all atrial locations was required to consider the map sufficient. A surface electrocardiography lead that demonstrated a dominant R-wave was used for reference annotation during point acquisition. No Confidense filters were applied (specifically, local activation time and cycle length stability).

After completing the high-density AF anatomic and point map, the Ripple map was viewed using a playback speed of 1 (this speed is an arbitrary parameter of the Ripple map program in which 1 is the slowest playback speed and 5 is the fastest). A rate of 1 corresponds to approximately 1% of real time. The lowest displayed voltage was set at 0.03 mV and the highest displayed voltage was set at 0.2 mV for viewing the Ripple map. The lower displayed voltage of 0.03 mV was necessary to correctly show regions of continuous low voltage electrograms. The upper boundary of 0.2 mV was chosen arbitrarily for map display, as the voltage was not used as a parameter to target for ablation. The Ripple window was prolonged to the maximum allowable duration of 2.5 seconds to allow for a complete display of all acquired electrograms.

HFRA was defined visually as regions of rapid and continuous Ripple activation. HFRA locations with the highest relative frequency by the visual analysis were targeted first, followed by progressively slower HFRA regions until termination. The highest frequency was explicitly defined concerning the atrium being mapped, rather than an absolute frequency. The largest anatomic regions measured on the mapping system (typically $>\sim$1.0-cm diameter) with HFRA were targeted for ablation first, followed by smaller areas. Isolated small segments, arbitrarily defined as <0.5-cm diameter, were not ablated, as these may have represented sheltered complex fractionated atrial electrograms.

Ablation Protocol

Ablation proceeded with PVI, followed by sequential ablation of the largest HFRA regions as described previously. Ablation of HFRA regions was performed in a cluster format and progressively expanded until local cycle length was observed to slow, and there was a loss of localized complex fractionated atrial electrograms and spatiotemporal dispersion. Ablation of HFRA sites was performed until AF termination occurred. Termination was determined solely by high-density electroanatomic maps with multielectrode catheters. There was no determination of rhythm etiology via surface tracings or far-field locations.

Termination as an endpoint was selected solely to test the hypothesis that HFRA sites were associated with acute AF maintenance. HFRA sites not necessary for AF termination were not subsequently ablated. If AF remained after ablation of all HFRA sites, up to 2 additional Ripple maps of the LA were performed, followed by a Ripple map of the right atrium. If AF persisted despite ablation of all HFRA regions in either chamber or if the HFRA regions were adjacent to a critical structure (eg, the AV node or sinus node), cardioversion was performed to restore NSR. Linear ablation of the LA roof was performed for induced or spontaneous roof-dependent macro–re-entrant atrial tachycardia (AT) or if extensive LA roof ablation was performed for HFRA in this location. Other linear or focal ablation was not performed unless a sustained AT was observed.

All patients underwent radiofrequency ablation using an externally irrigated, contact force sensing catheter (THERMOCOOL SMARTTOUCH and THERMOCOOL SMARTTOUCH SF; Biosense Webster). A minimum of 5 g contact was required before initiation of radiofrequency ablation. Power was fixed at 35 W and rarely increased to a

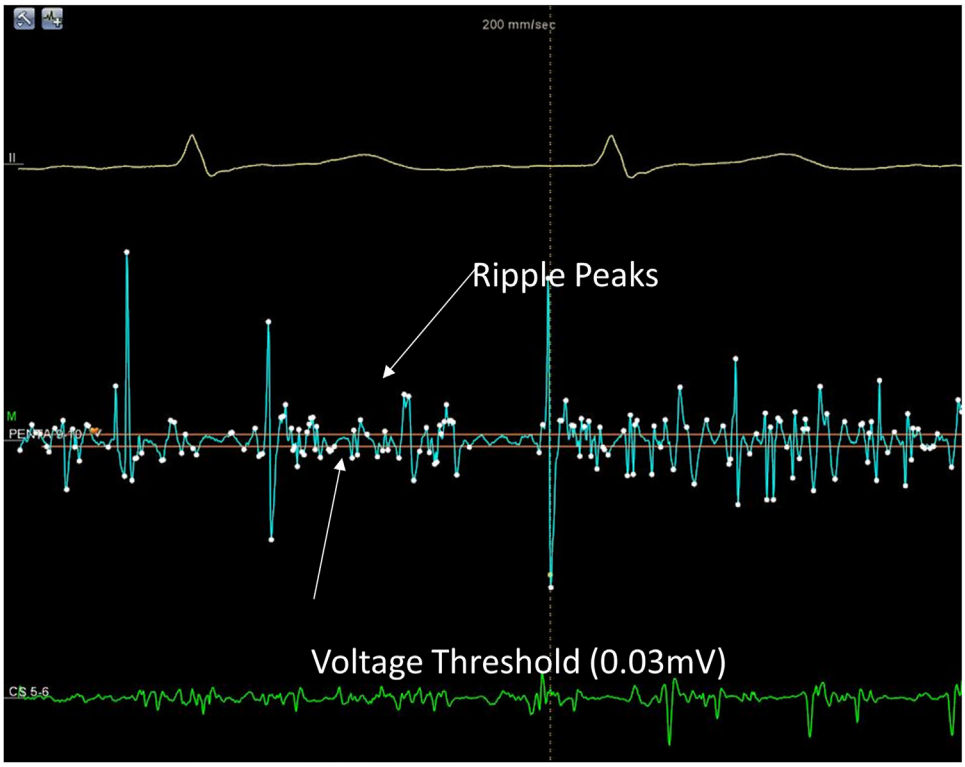

Figure 3 Example of Ripple frequency algorithm markers on an electrogram obtained during AF. The white markers represent a Ripple peak that was counted by the algorithm. The Orange lines delineate the preset voltage thresholds of ±0.03 mV from baseline 0 mV.

maximum of 45 W for 60 seconds if the LA roof or lateral mitral isthmus block could not be achieved. All linear lines performed were tested for conduction block. PV entrance block was evaluated 30 minutes after initial isolation was observed, and ablation was performed if needed to re-establish antral isolation. Esophageal temperature was monitored during posterior wall ablation (level 1 temperature probe; Smiths Medical, Dublin, OH). After restoring NSR (via ablation or cardioversion), an attempt to induce AT was performed with atrial pacing for up to 5 seconds in duration above the atrial effective refractory period or a minimum of 220 ms on 2 occasions. Repeat ablation procedures for AF were performed using the same strategy.

Ripple Frequency Analysis

The maps obtained from the original study were analyzed retrospectively using the Ripple frequency algorithm. The Ripple frequency map (Figure 2) displays the calculated values as a color-coded map with a dedicated color bar representing the range of observed frequencies to simplify analysis.

The Ripple frequency algorithm is an automated method for quantifying the number of directional changes in the Ripple-based voltage over time (dV/dT) above a preset amplitude threshold during the complete 2.5-second interval of the acquired point (Figure 3). The algorithm marks only positive or negative peaks when the signal is above the preset positive or negative threshold (typically 0.03 mV). The total peaks count for all algorithm-measured changes of the acquired electrogram was divided by 2.5 seconds to generate the Ripple frequency (defined as the Ripple peak count per second). The sites with the highest quartile of Ripple frequency within the LA, defined as the fastest 25% of all frequency measurements, were specified as the Ripple frequency regions of interest for further analysis.

To determine the sensitivity and specificity of the Ripple frequency algorithm, the LA was divided into 8 segments (PVs, posterior, inferior, septal, roof, anterior, base of the LA appendage, and lateral). Visual HFRA was utilized as the reference, and the highest quartile of the Ripple frequency map (75% or greater [ie, top 25%]) was then compared with the locations of visual HFRA. If 50% or more of the area identified with Ripple frequency overlapped with the visual HFRA reference, the site was determined to have correctly corresponded to the reference. The reference visual HFRA and Ripple frequency analysis were performed isolated from each other, and simultaneous side-by-side analysis was not performed. Ganglionated plexi (GP) were prespecified based on anatomic location and included the following: anterior right GP, inferior right GP, inferior left GP, superior right GP, and Marshall tract GP.[15] In the event that AF terminated with PV isolation, the Ripple frequency data were analyzed. However, these patients were not included in further analysis of Ripple frequency performance for identifying non-PV regions of interest.

Monitoring for rhythm outcomes was performed by clinical symptom assessment, routine electrocardiograms, and

Table 1 Characteristics of the patients at baseline (N = 84)

Characteristic	Ripple map strategy
Age, y	65.9 ± 10.3
Male	53 (63.1)
Structural heart disease*	11 (13.1)
Left atrial diameter, mm	44 ± 6
Ejection fraction, %	54.3 ± 9.7
Duration from first AF diagnosis, mo	37.4 ± 58.8
Duration uninterrupted AF before RFA, mo	5.1 ± 6.3
Medical history	
Diabetes	10 (11.9)
Hypertension	43 (51.2)
Stroke or transient ischemic attack	8 (9.5)
Vascular disease	16 (19.0)
CHA_2DS_2-VASc score	2.4 ± 1.6
Pacemaker or ICD	8 (9.5)
Preablation medications	
BB or CCB	74 (88.1)
Class Ic or III AAD	73 (86.9)
Class Ic AAD	23 (27.4)
Class III AAD	63 (75.0)
More than 1 AAD	11 (13.1)
DOAC or warfarin	73 (86.9)

Values are mean ± SD or n (%).

AAD = antiarrhythmic drug; AF = atrial fibrillation; BB = beta-blocker; CCB = calcium-channel blocker; CHA_2DS_2-VASc = congestive heart failure, hypertension, age ≥75 years, diabetes mellitus, prior stroke or transient ischemic attack or thromboembolism, vascular disease, age 65-74 years, sex category; DOAC = direct oral anticoagulation; ICD = implantable cardioverter-defibrillator; RFA = radiofrequency ablation.

*Congestive heart failure, constrictive pericarditis, amyloid cardiomyopathy, valvular cardiac surgery, hypertrophic cardiomyopathy.

Table 2 Ablation procedure results (N = 84)

Variable	Ripple map strategy
AF termination via RFA	74 (88.1)
Mode of termination	
NSR	9 (12.2)
AFL	30 (40.5)
Typical/CTI-dependent AFL	8 (11.0)
Focal AT	15 (20.3)
MAT	20 (27.0)
NSR via ablation	64 (76.2)
NSR via cardioversion	20 (23.8)
RFA time, min	
Total (all locations)	56.9 ± 18.4
Non-PV locations (including AT/AFL)	19.7 ± 15.7
Initial mean LA pressure, mm Hg	14.9 ± 4.7
CARTO atrial volume, mL	167.5 ± 44.1
RF Sites associated with AF termination	
PV antral isolation alone	11 (14.9)
Septal LA	47 (63.5)
LA roof	32 (43.2)
Inferior LA	29 (39.2)
Base of LAA	21 (28.4)
Lateral LA	21 (28.4)
Posterior LA	19 (25.7)
Anterior LA	18 (24.3)
Procedure duration, h	2.8 ± 0.7
Fluoroscopy time, min	1.2 ± 1.8
AF pace induced at procedure onset	16 (19.0)

Values are mean ± SD or n (%).

AF = atrial fibrillation; AFL = atrial flutter; AT = atrial tachycardia; CTI = cavotrcuspid isthmus; LA = left atrium/atrial; LAA = left atrial appendage; MAT = multifocal atrial tachycardia; NSR = normal sinus rhythm; PV = pulmonary vein; RFA = radiofrequency ablation.

when available, implanted device interrogation and ambulatory rhythm monitoring. Systemic, scheduled ambulatory rhythm monitoring was not performed. Rhythm outcomes included any atrial arrhythmia on or off antiarrhythmic drug (AAD), as well as AF on or off AAD and AT on or off AAD.

Continuous variables were compared using the Student's *t* test with a statistical significance preset at .05.

Results

Patients

Eighty-four consecutive patients underwent a first-time ablation for persistent AF using a Ripple map–guided approach. Baseline demographics are listed in Table 1. In these patients, the mean duration of uninterrupted AF before ablation was 5.1 ± 6.3 months. Structural heart disease was present in 13.1%. As determined by long-axis echocardiography, the mean LA diameter was 44 mm. LA enlargement (>40 mm) was present in 65.5% of patients. The mean CHA_2DS_2-VASc (congestive heart failure, hypertension, age ≥75 years, diabetes mellitus, prior stroke or transient ischemic attack or thromboembolism, vascular disease, age 65–74 years, sex category) risk score was 2.4 ± 1.6. In these patients, 73 (86.9%) of 84 had failed either a class Ic or class III antiarrhythmic medication, and 13.1% had failed more than 1 antiarrhythmic medication. Anticoagulation with either warfarin or a direct oral anticoagulant was administered before ablation in 73 (86.9%) of 84 patients.

Acute Procedure Characteristics and Outcomes

The mean procedure duration was 2.9 hours. At procedure onset, elevated mean LA pressure (>12 mm Hg) was present in 64.3% of patients (Table 2). AF was present at the procedure start in 44 (81.0%) of 54. Sustained AF was pacing-induced in 10 (19.0%) of 54 patients.

PVI was performed in all patients. Acute AF termination during the index ablation procedure was observed in 74 (88.1%) of 84 patients (14.9% with PVI alone and 75.1% with PVI plus nonantral ablation): 12.2% terminated to NSR, 29.7% to atypical, non–cavotrcuspid isthmus–dependent atrial flutter, 10.8% to typical cavotricuspid isthmus–dependent atrial flutter, 20.3% to focal AT, and 24.5% to multifocal AT. In those with AF termination, a mean of 2.8 ± 2.1 non-PV HFRA sites were ablated (Figure 4). Ablation of observed ATs was performed until sinus rhythm was restored in 64 (76.2%) of 84 patients. Cardioversion was performed to restore NSR for multifocal atrial tachycardia in 11 (13.1%) patients and AF in 9 (10.7%) patients. All other ATs were ablated until NSR was observed. Mapping and ablation were performed in the right atrium in 8 (9.5%) patients when AF did not terminate with LA ablation alone.

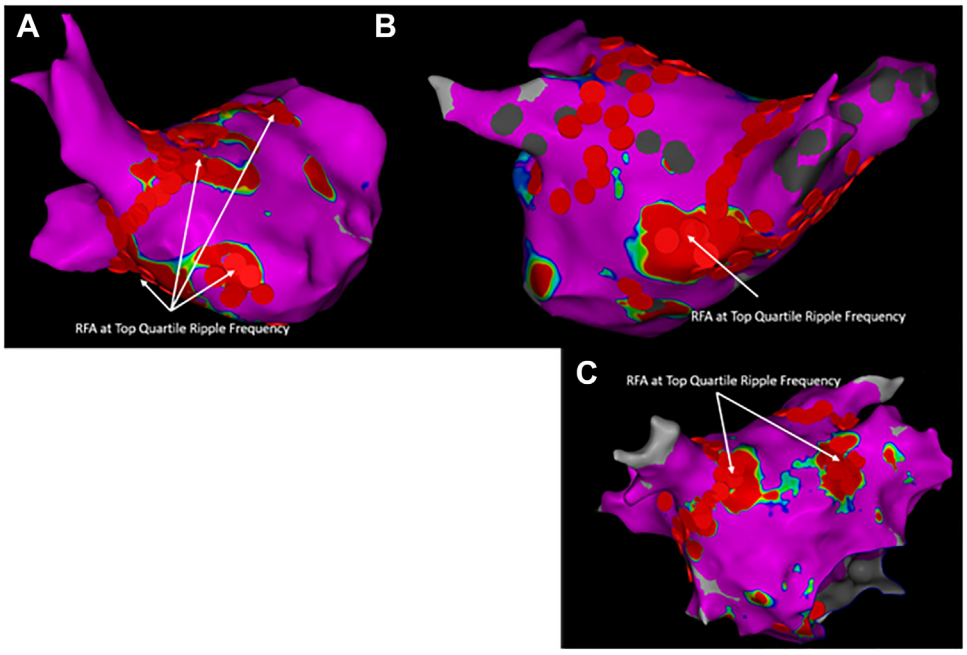

Figure 4 Examples of radiofrequency ablation lesion distributions. Ripple frequency maps in 3 patients undergoing first-time ablation for persistent atrial fibrillation (AF). Displayed are the Ripple frequency maps with the top quartile in red and the ablation lesions performed during the cases (red dot markers). **A:** The top quartile of Ripple frequency was observed at the left atrial septum inferior and superior as well as at the base of the left atrial appendage. Ablation at these sites resulted in AF termination to right atrial flutter. **B:** The top quartile of Ripple frequency was observed inferior left atrium adjacent to the right inferior pulmonary vein antrum. Ablation at this site resulted in AF termination to normal sinus rhythm. **C:** The top quartile of Ripple frequency was observed at the posterior superior septum adjacent to the right superior pulmonary vein antrum as well as the base of the left atrial appendage. Ablation at these sites resulted in AF organization to mitral isthmus–dependent flutter.

There were no major procedural complications (transient ischemic attack, cerebrovascular accident, pericardial effusion, atrioesophageal fistula) within 30 days of the initial ablation.

Ripple Frequency Results

A total of 115 maps with 348,748 points from 84 patients were analyzed using the Ripple frequency algorithm. The mean point density was 14.3 ± 9.9 per cm^2 (Table 3). The mean number of maps per patient was 1.4 ± 0.6. The highest quartile of Ripple frequency was present in non-PV sites necessary for AF termination with a 90.2% sensitivity and 86.5% specificity. The most common non-PV sites associated with AF termination were the LA septum 63.5%, LA roof region 43.2%, and inferior LA 39.2%.

The maximum Ripple frequency observed was 115.4 ± 25.2 (range, 58–191) per second. The highest quartile of Ripple frequency started at 81.8 (range, 31.5–111.8) per second. The Ripple frequency decreased significantly after the ablation of regions observed on the initial map compared with subsequent maps (115.4 ± 25.2 per second vs 100.9 ± 26.0 per second; $P = .006$).

The mean number of atrial regions per map containing the highest quartile of Ripple frequency was 4.6. The highest quartile of Ripple frequency comprised a surface area of 11.6 ± 10.2 (range, 0.6-38.1) cm^2, encompassing 5.6 ± 5.1% of the total atrial surface area with a range of 0.3% to 20.1%.

The most common region demonstrating Ripple frequency in the highest quartile in 90.4% of patients was the left side of the interatrial septum. The inferior LA (66.7%), PV antrum (65.5%), and the base of the LA appendage (61.9%) were the next most common. GPs were common anatomic locations to observe high Ripple frequency. The highest quartile of Ripple frequency was noted in 83 (98.8%) of 84 patients at 1 of the 5 GP locations. In addition, the GPs comprised 44.9% of the total locations.

The highest quartile of Ripple frequency sites exhibited a 96.7% sensitivity and 91.1% specificity for correctly identifying atrial regions identified with visual HFRA analysis.

Efficacy Outcomes

After a mean follow-up of 14.0 ± 6.5 months, as documented by symptoms, electrocardiogram, Holter monitor, or device interrogation, 78 (92.9%) of 84 patients were free of AF, 70 (83.3%) of 84 patients were free of either focal AT or atrial flutter, and 67 (79.8%) of 84 patients were free of any sustained atrial arrhythmia (Table 4). A mean number of 1.2 ablation procedures were performed per patient. The second ablation was performed after 8.4 ± 4.7 months following the first procedure. Cardioversion was required for sustained AF or AT within 90 days of the index ablation in 17.6% of patients. At the last follow-up, 30.9% of patients remained on antiarrhythmic therapy.

Table 3 Ripple frequency results (N = 84)

Result	Ripple frequency strategy
Number of acquired points analyzed (all patients)	348,748
Acquired point density, points per cm^2	14.3 ± 9.9
AF Ripple frequency maps performed	1.4 ± 0.6
1	54 (64.3)
2 or 3	30 (35.7)
Maximum Ripple frequency, map #1	115.4 ± 25.2
Maximum Ripple frequency, map #2/#3	100.9 ± 26.0
Ripple frequency range	0–191
Highest-quartile Ripple frequency range	81.8 ± 22.4–115.4 ± 25.2
Number of atrial regions highest-quartile Ripple frequency	4.6 ± 1.8
Location of LA regions with highest-quartile Ripple frequency (n = 82 maps)	
Septal	76 (90.4)
Inferior	56 (66.7)
PV antrum	55 (65.5)
Anterior base of LAA	52 (61.9)
Anterior	45 (53.6)
Roof	43 (51.2)
Posterior	40 (47.6)
Lateral	32 (38.1)

Values are n, mean ± SD, or n (%).

AF = atrial fibrillation; LA = left atrial; LAA = left atrial appendage; PV = pulmonary vein;

Table 4 Follow-up observations (N = 84)

Variable	Ripple Map Strategy
Follow-up duration, d	406 ± 141
Freedom from documented arrhythmia	
AF	78 (92.9)
AT/AFL	70 (83.3)
Any atrial arrhythmia	67 (79.8)
Additional ablation performed for AF or AT/AFL	15 (22.0)
Number of ablations performed per patient	1.2 ± 0.4
Cardioversion for AF or AT/AFL within 90 days of index ablation	15 (17.9)
AAD at last follow-up	18 (26.4)
Holter performed or implanted device present	26 (31.0)

Values are mean ± SD or n (%). Freedom from any atrial arrhythmia, as well as AF and AT/AFL were determined on or off AADs.

AAD = antiarrhythmic drug; AF = atrial fibrillation; AFL = atrial flutter; AT = atrial tachycardia.

Discussion

Main Findings

This study evaluated a novel algorithm designed to quantify Ripple map–based changes in the bipolar electrogram. The key findings were the following: (1) the highest quartile of Ripple frequency was present in non-PV sites associated with AF termination with a 90.2% sensitivity and 86.5% specificity; (2) the Ripple frequency algorithm had high sensitivity and specificity for identifying reference HFRA locations in persistent AF patients; and (3) over an 18-month follow-up period, ablation of HFRA sites was associated with a 92.9% freedom from AF and a 79.8% freedom from AT or AF after a median of 1.2 ablation procedures. These findings support a potential association between Ripple frequency and critical areas of the atrium necessary for AF maintenance and possible recurrence. The mean atrial surface area comprising the highest Ripple frequency was a modest 5%, indicating that extensive ablation may not be necessary to adequately eliminate regions of the atrium important for AF maintenance and recurrence risk.

Other Observations

In prior studies, a Ripple map has been utilized to identify repetitive focal and re-entrant activation during sustained AF[16] and abnormal atrial potentials during sinus rhythm in nonparoxysmal AF.[17] In these studies, ablation of identified regions of interest on the Ripple map resulted in improved termination of AF and freedom from AF during the 12 months of follow-up. These studies differ from our current study regarding the Ripple frequency algorithm in 2 respects. The Ripple frequency algorithm is quantitative, in contrast to the visual observations used to identify repetitive wavefronts or abnormal atrial potentials. Secondly, Ripple frequency does not perform wavefront analysis; instead, it measures predefined electrogram characteristics.

High-density, precise mapping of Ripple frequency in patients with persistent AF may provide insights into regions of the atrium necessary for supporting AF. We found in this study that multiple locations (eg, LA septum, LA inferior) more often contained high Ripple frequency than the PV antrum. This supports prior observations of infrequent AF termination with PVI alone.[6] The atrial characteristics observed with Ripple frequency had wide variability between patients, with peak Ripple frequency ranging from 58 to 191 per second, suggesting significant interpatient differences in the pathophysiology and underlying substrate of persistent AF. In addition, GPs often demonstrated high Ripple frequency, with 98.8% of patients exhibiting at least 1 GP in the top quartile of Ripple frequency. In our study, however, non-GP locations associated with AF maintenance were more common than GP locations and may help explain the mixed outcomes with GP ablation alone.[18]

The Ripple frequency algorithm provides a relatively simple, quantitative assessment of regions of interest during AF, spatially located efficiently on a 3-dimensional electroanatomic CARTO 3 map.

Limitations

Several limitations restrict the scope of this study's findings. This was a single-center retrospective study, and multicenter evaluation is needed to improve the determination of the algorithm's efficacy. In addition, the algorithm's calculated sensitivity and specificity were based on a reference visual

Ripple analysis. Visual estimation lacks the quantitative precision necessary for a true reference and has the potential for observer bias. Systematic outpatient telemetry monitoring was not performed, so the arrhythmia recurrence may have been underestimated. The right atrium was not routinely mapped at baseline, and therefore this study may underestimate the importance of high-frequency sites in this chamber. We also acknowledge that the stability of Ripple activation sites of interest prior to PVI has not been established, and may in at least a subset of patients, result in inaccurate localization. It is reasonable that future studies using this technique may benefit from Ripple mapping after PVI is complete. Finally, this work's retrospective nature does not allow conclusions to be drawn regarding the outcomes of using the Ripple frequency algorithm prospectively to determine ablation targets.

Conclusion

This study supports the potential that a novel automated analysis of Ripple frequency may provide a complementary method to existing techniques such as spatiotemporal dispersion analysis to identify regions of interest in persistent AF.

Funding Sources: The authors have no funding sources to disclose.

Disclosures: Daniel Melby receives honoraria from Biosense Webster for educational and board member activities. No other author has disclosures.

Authorship: All authors attest they meet the current ICMJE criteria for authorship.

Patient Consent: All patients consented to research participation.

Ethics Statement: Institutional Review Board approval was obtained, and the research reported in this paper adhered to the Helsinki Declaration guidelines.

References

1. Mou L, Norby FL, Chen LY. Lifetime risk of atrial fibrillation by race and socioeconomic status: ARIC study (Atherosclerosis Risk in Communities). Circ Arrhythm Electrophysiol 2018;11:e006350.
2. Haïssaguerre M, Jaïs P, Shah DC, et al. Spontaneous initiation of atrial fibrillation by ectopic beats originating in the pulmonary veins. N Engl J Med 1998; 339:659–666.
3. January CT, Wann LS, Alpert JS, et al. 2014 AHA/ACC/HRS Guideline for the management of patients with atrial fibrillation: a report of the American College of Cardiology/American Heart Association Task Force on Practice Guidelines and the Heart Rhythm Society. J Am Coll Cardiol 2014;64:e1–e76.
4. Natale A, Reddy VY, Monir G, et al. Paroxysmal AF catheter ablation with a contact force sensing catheter: results of the prospective, multicenter SMART-AF trial. J Am Coll Cardiol 2014;64:647–656.
5. Reddy VY, Dukkipati SR, Neuzil P, et al. A randomized controlled trial of the safety and effectiveness of a contact force sensing irrigated catheter for ablation of paroxysmal atrial fibrillation: results of the TOCCASTAR study. Circulation 2015;132:907–915.
6. Aryana A, Singh SM, Kowalski M, et al. Acute and long-term outcomes of catheter ablation of atrial fibrillation using the second-generation cryoballoon versus open-irrigated radiofrequency: a multicenter experience. J Cardiovasc Electrophysiol 2015;26:832–839.
7. Verma A, Jiang C, Betts TR, et al. Approaches to catheter ablation for persistent atrial fibrillation. N Engl J Med 2015;372:1812–1822.
8. Calkins H, Kuck KH, Cappato R, et al. 2012 HRS/ EHRA/ECAS expert consensus statement on catheter and surgical ablation of atrial fibrillation: recommendations for patient selection, procedural techniques, patient management and follow-up, definitions, endpoints, and research trial design: a report of the Heart Rhythm Society (HRS) Task Force on Catheter and Surgical Ablation of Atrial Fibrillation. Developed in partnership with the European Heart Rhythm Association (EHRA), a registered branch of the European Society of Cardiology (ESC) and the European Cardiac Arrhythmia Society (ECAS); and in collaboration with the American College of Cardiology (ACC), American Heart Association (AHA), the Asia Pacific Heart Rhythm Society (APHRS), and the Society of Thoracic Surgeons (STS). Heart Rhythm 2012;9:632–696.
9. Morillo CA, Klein GJ, Jones DL, Guiraudon CM. Chronic rapid atrial pacing. Structural, functional, and electrophysiological characteristics of a new model of sustained atrial fibrillation. Circulation 1995;91:1588–1595.
10. Vaquero M, Calvo D, Jalife J. Cardiac fibrillation: from ion channels to rotors in the human heart. Heart Rhythm 2008;5:872–879.
11. Shivkumar K, Ellenbogen KA, Hummel JD, Miller JM, Steinberg JS. Acute termination of human atrial fibrillation by identification and catheter ablation of localized rotors and sources: first multicenter experience of focal impulse and rotor modulation (FIRM) ablation. J Cardiovasc Electrophysiol 2012; 23:1277–1285.
12. Narayan SM, Krummen DE, Shivkumar K, Clopton P, Pappel WJ, Miller JM. Treatment of atrial fibrillation by the ablation of localized sources: CONFIRM (Conventional Ablation for Atrial Fibrillation With or Without Focal Impulse and Rotor Modulation) trial. J Am Coll Cardiol 2012;60:628–636.
13. Seitz J, Bars C, Théodore G, et al. AF Ablation guided by spatiotemporal electrogram dispersion without pulmonary vein isolation: a wholly patient-tailored approach. J Am Coll Cardiol 2017;69:303–321.
14. Melby DP, Gornick C, Abdelhadi R, et al. Outcomes following persistent atrial fibrillation ablation using localized sources identified with Ripple map. J Cardiovasc Electrophysiol 2019;30:1860–1867.
15. Stavrakis S, Po S. Ganglionated plexi ablation: physiology and clinical applications. Arrhythm Electrophysiol Rev 2017;6:186–190.
16. Takahashi Y, Iwai S, Yamashita S, et al. Novel mapping technique for localization of focal and reentrant activation during atrial fibrillation. J Cardiovasc Electrophysiol 2017;28:375–382.
17. Nakatani Y, Yamaguchi Y, Sakamoto T. Ripple map guided catheter ablation targeting abnormal atrial potentials during sinus rhythm for non-paroxysmal atrial fibrillation. J Cardiovasc Electrophysiol 2020;31:1970–1978.
18. Kampaktsis PN, Oikonomou EK, Choi DY. Efficacy of ganglionated plexi ablation in addition to pulmonary vein isolation for paroxysmal versus persistent atrial fibrillation: a meta-analysis of randomized controlled clinical trials. J Interv Card Electrophysiol 2017;50:253–260.